Liquid Crystalline Rod−Coil Block Copolymers by Stable Free Radical Polymerization: Synthesis, Morphology, and Rheology

Padma Gopalan, Yuanming Zhang, Xuefa Li, Ulrich Wiesner, and Christopher K. Ober*

Department of Materials Science and Engineering, Cornell University, Ithaca, New York 14853

Received October 10, 2002; Revised Manuscript Received February 20, 2003

ABSTRACT: We have synthesized and characterized rod−coil diblock, triblock, and starblock copolymers of controlled molecular weight by stable free radical polymerization, where the rod part consists of "mesogen jacketed liquid crystalline segments" (MJLCP). The MJLCP segment examined in our studies is poly{2,5-(4-butylbenzoyl)oxystyrene} (PBBOS) while the coil part is poly(styrene). SAXS studies of the block copolymers at room temperature predominantly show only a first-order maximum in their SAXS spectra. Above the T_g of the two blocks (∼150 °C) no phase-separated morphology could be detected in temperature-dependent SAXS measurements of the block copolymers. Slow cooling regenerates the morphology, indicating very slow ordering kinetics. The effects of variation in molecular architecture and increasing topological constraint in going from homopolymer to star block copolymer on melt rheology (i.e., viscosity, relaxation times, and activation energies) are reported. In the master curves of all the block copolymers and homopolymers studied, nonterminal behavior was observed at low shear frequencies along with the absence of an entanglement plateau. In the PBBOS homopolymer an increase in molecular weight resulted in a decrease in the modulus of the nematic phase that was associated with a greater extent of shear orientation. On varying the molecular architecture from homopolymer to diblock to starblock copolymer, a decrease in the complex viscosity was observed that is attributable to the presence of polystyrene as the second block and the effect of topological constraints on molecular relaxation. The activation energies also follow the same trend as complex viscosity and relaxation times.

Introduction

Side chain LC polymers (SCLCP's) with mesogenic groups laterally attached to the polymer backbone constitute a distinct class of liquid crystals. Unlike the conventional SCLCPs with end-on attachment of mesogens, lateral attachment of mesogens hinders the rotational motion along the long axis of the rods. Weissflog et al.[1] synthesized the first such SCLCP. Since then, a number of laterally attached side chain LCPs have been reported including poly(siloxanes),[2] poly(acrylates),[3] and norbornene derivatives.[4] All these polymers have a flexible linker connecting the mesogen to the backbone. The family of SCLCPs with laterally attached mesogenic groups was further extended by Zhou et al. to "mesogen-jacketed liquid crystal polymers" (MJLCPs).[5a] MJLCPs have mesogenic groups attached laterally to the polymer backbone through their center of gravity without any spacers or with very short spacers. The lack of spacers leads to an extended LC region in the polymer and properties similar to semirigid main chain LC polymers. In most of the SCLCPs, if there are no flexible spacers, the motion of the mesogenic side groups is directly coupled to the motion of main chain segments, preventing any LC orientation.[6] However, MJLCPs form a nematic liquid crystalline phase even in the absence of a critical length of flexible spacer. Many MJLCPs reported to date are based on 2,5-disubstituted vinylhydroquinone. For example, 2,5-bis[(4-butylbenzoyl)oxy]-styrene (BBOS) has rigid and bulky benzoate groups at the 2,5-positions of the phenyl ring.[5a] Despite these bulky substituents, BBOS polymerizes efficiently under both conventional[5a] and stable free radical[7] polymerization conditions. MJLCPs of the type poly[di(cyclohexyl)vinyl terephthalate] have been reported, which do not have rigid-rod mesogenic groups but are liquid crystalline. Their liquid crystallinity may be attributed to the strong steric interactions among the side groups and between the side groups and the main chain segments.[5b] In recent work the authors have synthesized poly[di(4-heptyl)vinyl terephthalate] and reported the formation of a hexagonal columnar LC phase. This supramolecular hexagonal columnar phase, according to the authors, is formed by pendent nonmesogenic templates and has the highest liquid crystalline order observed in MJLCPs so far. The unique molecular design of MJLCP's induces liquid crystallinity even in polymers which lack the conventional characteristics of rigid segments and the presence of flexible spacers.[5c]

Our interest in MJLCPs is to design rod−coil block copolymers with the rod part consisting of the MJLCP. The unique molecular design of MJLCPs could potentially lead to different morphologies than those observed to date in rod−coil systems. To synthesize these rod−coil polymers, we must consider that most of the mesogenic groups contain functional groups (such as ester or amide links) which limits synthetic strategy. Typically, anionic polymerization has been used to synthesize rod−coil block copolymers.[5d] This choice limits the selection of monomers to anionically polymerizable monomers and excludes many highly functional monomers owing to significant side reactions. Stable free radical polymerization (SFRP) would be an ideal technique to apply to the synthesis of a wider range of functionalized rod−coil block copolymers[8] as it offers the ease of free radical polymerization with other features of living polymerization such as the synthesis of a variety of star and block architectures.[9] Recently, Zhou et al. have used SFRP to synthesize rod−coil diblock copolymers of poly{styrene-*b*-2,5-bis[4-methoxyphenyl]oxycarbonyl}styrene}.[10] They also studied the self-assembly behavior in dilute solution by both

10.1021/ma021573u CCC: $25.00
Published on Web 04/08/2003

static and dynamic light scattering techniques and reported a core and shell structure in xylene, a nonsolvent for the rod.

It is interesting to examine the melt flow behavior of the MJLCPs, given their unique molecular architecture. To date, neither mechanical property studies nor rheological studies have been performed on MJLCPs. SCLCPs with laterally fixed mesogenic groups are relatively new and have not been studied widely. To the best of our knowledge, the only work on the rheology of liquid crystals with side-on fixed mesogenic groups has been reported by Berghausen and co-workers.[13] They examined a nematic side-group liquid crystalline polymer with polymethacrylate backbone and a hydroquinone bis(benzoate) mesogen coupled laterally through a spacer of 11 methylene units. Compared to the end-on mode SCLCPs, these researchers found that the side-on type could not be aligned by large-amplitude oscillatory shear and that the master curves of G' and G'' did not show any plateau modulus, indicating lack of entanglements for the molecular weights examined.

Our earlier studies on the polymerization behavior of laterally attached mesogens such as 2,5-bis(4-butylbenzoyl)oxystyrene (BBOS) under SFRP conditions showed unusually high reactivity compared to other styrenics and by varying the reaction time good control of molecular weight could be achieved.[7,11] On the basis of these observations, here we report the synthesis of selected molecular architectures including diblock, starblock, and ABA triblock polymers of MJLCP segments with polystyrene. The bulk morphology of these systems is studied using cross-polarized optical microscopy, wide- and small-angle X-ray scattering (WAXS and SAXS), and transmission electron microscopy (TEM). Furthermore, their basic rheological properties were examined in order to study the effects of molecular architecture and increasing topological constraint on their dynamic behavior.

Experimental Section

Polymer Characterization. A Varian XL 400 NMR using chloroform-*d* as solvent with tetramethylsilane as internal standard was used to obtain the NMR spectra of all the compounds. Thermal analysis was carried out under nitrogen atmosphere by means of Perkin-Elmer DSC 7 and TGA 7 instruments at a heating rate of 10 °C/min. Measurements of both molecular weight and polydispersity of all polymer samples were carried out using Waters Ultrastyragel HT columns operating at 40 ° C. THF was used as the solvent, and the GPC was operated at 1 mL/min. Solution concentrations of 1 mg/mL for PBBOS, 2 mg/mL for PDAS, and solution volumes of 50 μL were employed. Molecular weights were calculated from GPC elution volume data using monodisperse polystyrene standards.

Morphology Examinations. Bulk samples were cast from 5 wt % toluene solution by slow evaporation over 1 week and then annealed at 150 °C for 4 days under high vacuum followed by slow cooling over 6 h. Cross-polarized optical microscopy (POM) and a hot stage were used to examine the temperature dependence of liquid crystallinity in the samples. Morphologies were examined by a combination of wide- and small-angle X-ray scattering (WAXS and SAXS), at room temperature and at elevated temperatures, as well as by transmission electron microscopy (TEM). For TEM studies, a piece of bulk sample was embedded into epoxy, which was cured at 70 °C for 7 h. Microtomy was then carried out with a Leica ultramicrotome to produce the cross-sectioned thin film specimen (~70 nm thick). A JEOL 1200 TEM with an accelerating voltage of 120 keV was used for imaging.

Synthesis. *BBOS Monomer.* The monomer 2,5-bis[(4-butylbenzoyl)oxy]styrene, BBOS (Figure 1), was synthesized by the reaction of 2-vinyl-1,4-dihydroxybenzene and 4-butylbenzoyl chloride according to the method described by Zhou et al.[5a] ^{1}H NMR ($CDCl_3$): δ = 0.95, 6H for $CH_3{}^a$, 1.35, 4H for $CH_2{}^b$, 1.65, 4H for $CH_2{}^c$, 2.70, 4H for $CH_2{}^d$, 5.10−5.90, 2H for $=CH_2{}^e$, 6.60−6.95, 1H for $-CH^f=$ and 7.00−8.30, 11H for the phenylene rings. As reported earlier,[5a] BBOS exhibits a smectic phase between its melting temperature 68 °C and clearing temperature 95 °C.

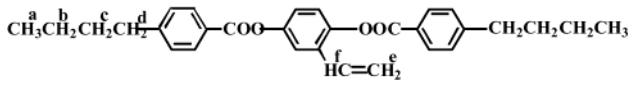

(1)

Figure 1. Structure of [4-butylbenzoyloxy]styrene (BBOS).

Polystyrene Macroinitiators. Three different TEMPO-based initiators were used as shown in Figure 2. These are (a) unimer with one initiating site which generates diblock copolymers, (b) diarm initiator with two initiation sites which generates triblock copolymers, and (c) star initiator with three initiating sites which generates starblock copolymers.

In all the block copolymers synthesized in this series, styrene was used as the first block; therefore, the first step is the synthesis of macroinitiator from the three different initiators. In a typical procedure styrene was mixed with the required amount of one of the above initiators in a Schlenk flask containing a magnetic stir bar. The reaction mixture was purged with nitrogen and subjected to four freeze−thaw cycles to remove any dissolved oxygen and sealed under vacuum. The flask was placed directly into an oil bath preset at 130 °C. Typically, polymerizations were carried out for 50−75 h depending on the desired molecular weight. The macroinitiator was isolated by repeated precipitation in methanol and dried under vacuum overnight.

Homopolymer of BBOS (PBBOS). Homopolymer of BBOS was synthesized by typically mixing 300 mg (0.65 mmol) of BBOS with 6.86 mg of uniarm initiator (0.026 mmol) in a 2 mL ampule containing a magnetic stir bar. The polymerization mixture was purged with N_2, subjected to four cycles of freeze−thaw, and sealed under vacuum. The sealed ampule was placed in a preheated oil bath at 125 °C and polymerized for 8 h. The reaction mixture was precipitated in methanol and purified by column using dichloromethane as solvent to obtain a BBOS homopolymer of M_n 5800 and PDI 1.30.

Block Copolymers. The block copolymers were synthesized using uniarm, diarm, and star polystyrene macroinitiators and polymerizing them in a predetermined ratio with BBOS. Block copolymerization was carried out in a solvent and not in bulk. Solvents such as xylene, benzene, and *o*-dichlorobenzene were examined, and it was found that the polymerization was best controlled in *o*-dichlorobenzene, as it maintains good solubility for the blocks throughout the polymerization and has a low transfer constant. In a typical procedure copolymerization was carried out in two-necked Pyrex ampules sealed under reduced pressure. Different ratios of the polystyrene macroinitiator were mixed with the liquid crystalline monomer in *o*-dichlorobenzene and polymerized at 125 °C for 2−3 days. For example, 41.8 mg of star PS macromonomer (M_n 19 000, PDI 1.18) was mixed with 200 mg of BBOS (0.4 mmol) and 0.5 mL of *o*-dichlorobenzene. This mixture was subjected to four cycles of freeze−thaw and reacted for 48 h. The polymerization mixture was precipitated in methanol and subsequently purified by column chromatography using dichloromethane as eluant to remove residual monomer. The block copolymer was further extracted with acetone to remove dead polystyrene macroinitiator. This gave a starblock copolymer of M_n 40 980. In the ^{13}C spectra additional peaks for the ester carbonyl at 166 ppm between 10 and 50 ppm for the butyl substituent along with the ^{1}H NMR and GPC data confirm the block nature (Figure 3).

Rheological Measurements. Samples for rheological measurements were prepared into 13 mm diameter (1 mm thickness) disks at 100 °C and 5 psi pressure in a hot press. These disks were annealed at 110 °C for a day under vacuum. All the samples were held at 180 °C for 10 min prior to the

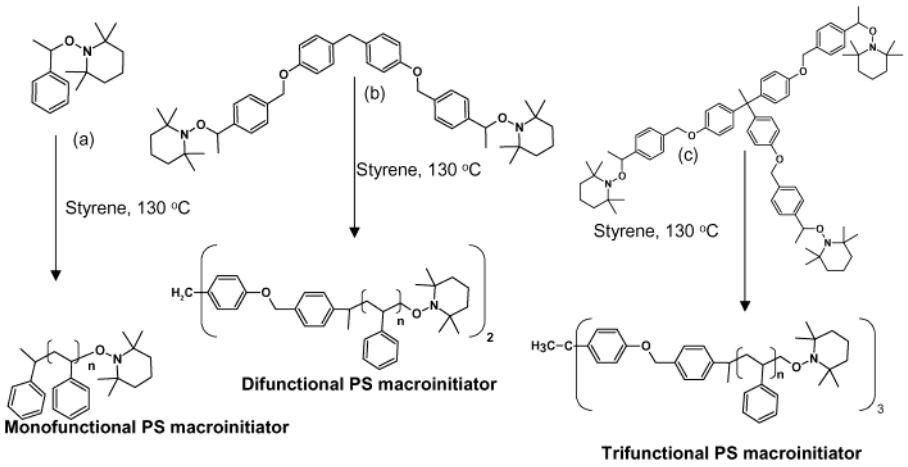

Figure 2. Synthetic scheme for polystyrene macroinitiators from (a) unimer or uniarmed, (b) diarmed, and (c) triarmed alkoxyamine initiators.

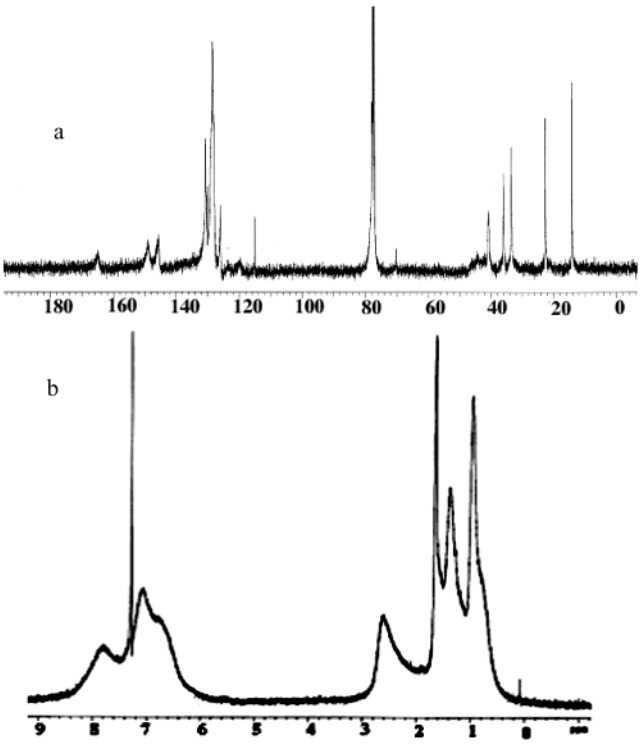

Figure 3. (a) ^{13}C NMR and (b) ^{1}H NMR of PS-*b*-PBBOS diblock copolymer.

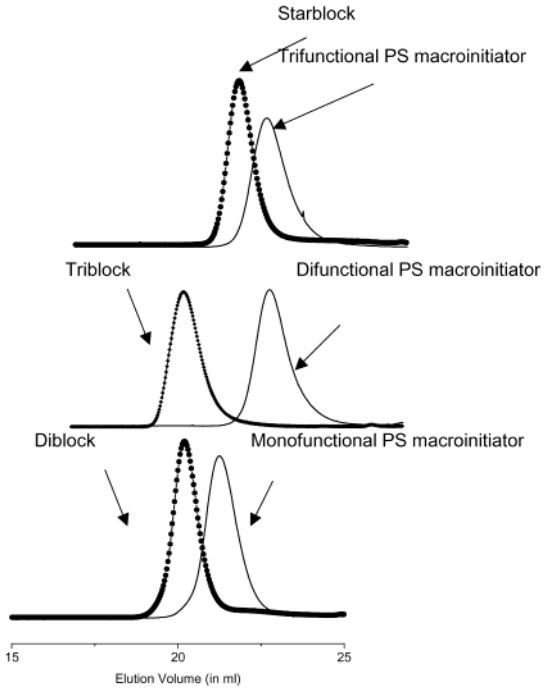

Figure 4. Representative GPC plots for diblocks, triblocks, and starblocks of PS with PBBOS along with the corresponding macroinitiators.

experiments. A Rheometrics ARES rheometer was used for the measurements. The experimental temperature was controlled by using forced N_2 gas convection with integral and proportional plus derivative controller. The temperature control was within ±0.5 °C. A parallel-plate geometry (diameter = 13 mm, gap = 1 mm) was used in studying the temperature dependence of the apparent shear viscosity at a fixed rim shear rate. Measurements were performed at temperatures spaced every 5 °C in the temperature range 100−200 °C. Dynamic temperature sweep experiments were also performed using the same setup.

Results and Discussion

Synthesis. As in all radical polymerizations, oxygen can adversely affect polymer formation of MJLC monomers. The critical step in successful polymerization is removal of oxygen via freeze−thaw cycle followed by N_2 purge to remove any dissolved oxygen. Purity of the liquid crystalline monomer was also found to be an important factor for narrow polydispersity. Hence, BBOS monomer was purified by column chromatography and recrystallized twice from petroleum ether. All the polymerizations were carried out in *o*-dichlorobenzene as solvent. Better control over the polymerization was obtained by using 50 wt % solutions of the monomer and macroinitiator for polymerization. Higher wt % concentration of monomer led to faster polymerization but larger polydispersity in the sample. BBOS block copolymers were found to be soluble both at room temperature and at 125 °C; it is also possible to directly dissolve the PS macroinitiators in a BBOS melt at 95 °C (above the clearing temperature of BBOS) and perform the polymerization without solvent at 125 °C; however, the polydispersities obtained are higher (1.15−1.45) compared to that of polymer formed by solution polymerization.

Figure 4 shows representative GPC plots for diblocks, triblocks, and starblocks of BBOS with styrene. Compared to the starting PS macroinitiator, a clean uni-

Table 1. Specifications of Various Block Copolymers of PS and PBBOS Synthesized in Our Study

sample ID[a]	PS macroinitiator M_n (g/mol)	M_n of block copolymer (g/mol)[b]	PDI	mol % rod unit[c]	LC[d]
BD1	6140	19 890	1.35	34	√
BD2	6140	13 840	1.30	22	√
BD3	10350	18 500	1.22	15	X[e]
BD4	12370	26 155	1.15	20	√
BT1	3570	30 400	1.34	63	√
BT2	8870	18 160	1.26	19	√
BS1	19070	40 980	1.14	21	√
BS2	8620	16 530	1.21	17	√

[a] BD stands for PS-*b*-PBBOS diblock, BT for PBBOS-*b*-PS-*b*-PBBOS triblock, and BS for PS-*b*-PBBOS starblock copolymer. [b] Measured by GPC using polystyrene as standard and THF as eluant. [c] Calculated based on GPC molecular weights. [d] Phase behavior as observed by polarized optical microscopy. [e] X: observed only by WAXS.

modal shift to higher molecular weight is seen in all three block copolymers shown in the figure. The living nature of these chains was confirmed by sequential addition of a second monomer like styrene. The unimodal distribution in GPC along with the presence of aromatic peaks from both BBOS and PS block in the ^{1}H and ^{13}C NMR spectra (Figure 3) confirms the block nature.

Morphology. *Liquid Crystalline Phase Behavior.* As reported earlier, BBOS monomer has a melting temperature of 68 °C and a clearing temperature of 98 °C. It exhibits a smectic LC phase between 68 and 98 °C. The polymer as such is found to be nematic above its T_g, i.e., 130 °C, with no detectable clearing temperature.[5a]

Most of the diblock, starblock, and ABA triblock copolymers of BBOS and styrene listed in Table 1 showed birefringence when observed by POM. On heating the block copolymers above 130 °C, birefringence develops with no observable clearing temperature. Diblock copolymers for which no liquid crystallinity was observable by POM had less than 15 mol % of the LC block. This observation is in agreement with similar reports by Zhou et al.[7] where they found Schlieren textures for block copolymers with 26 and 36 mol % of LC units. The presence or absence of birefringence as observed by POM is recorded in Table 1. Wide-angle X-ray studies on solvent-cast block copolymer films give more definitive information about the nematic liquid crystalline phase. Figure 5 shows intensity, I, vs 2θ plots for some of the block copolymers. In all cases, i.e., irrespective of chain architecture, we see a peak between 19 and 20 Å (2θ = 4−5°) that corresponds to an interchain packing distance that is close to that observed for fibers drawn from BBOS homopolymers (17.2−18 Å). A second broader peak between 4 and 5 Å (2θ = 19−20°) represents the intermolecular distance between the mesogenic units.[7]

Microphase Separation. Small-angle X-ray scattering (SAXS) was used to examine the microphase-separated morphology of the diblock and starblock copolymers at various temperatures. Results for two representative samples are shown in Figure 6. Their molecular weights and compositions are listed in Table 2. These polymers were prepared using the same methods as those polymers reported in Table 1. At room temperature (see the top curves in Figure 6a,b), both the block and starblock copolymers show only one peak in their SAXS spectra, at 0.39 nm^{-1} for the diblock and at 0.29 nm^{-1} for the starblock copolymer. This suggests that the block copolymers are phase-separated with a structural d spacing of 16 and 21.5 nm for the diblock and starblock copolymer, respectively. The absence of higher order peaks indicates that, even after slow and careful solvent casting, the composition profile across the interface is rather smooth, and/or no significant long-range order of the microphase separated structures could be estab-

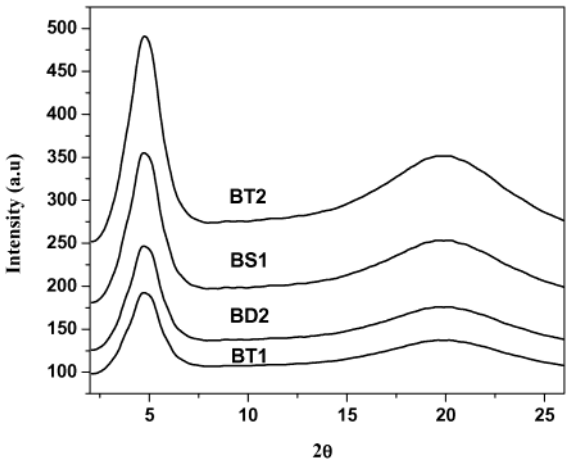

Figure 5. WAXS plots of intensity vs 2θ for some of the diblocks, triblocks, and starblocks of poly(styrene) with poly-[(4-butylbenzyloxy)styrene] (PBBOS).

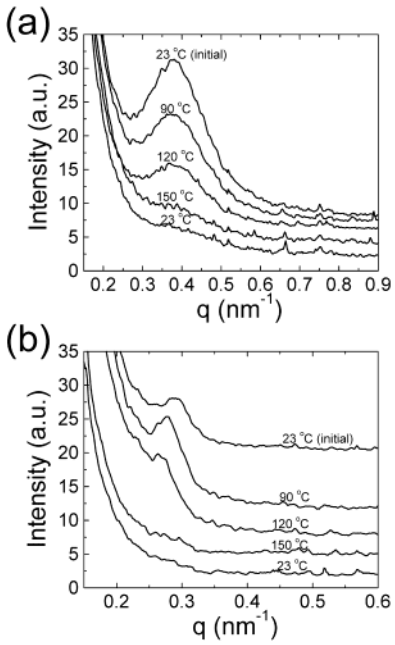

Figure 6. Temperature-dependent SAXS data of (a) a diblock and (b) a starblock PS−PBBOS copolymer. Temperatures of SAXS measurements are labeled above the corresponding curves. The top curves labeled with 23 °C (initial) are the room temperature results of initial samples prepared through very slow solvent casting procedure described in the Experimental Section. The bottom curves labeled with 23 °C are the results after the samples were heated to 150 °C and cooled to room temperature subsequently.

Table 2. Molecular Weight and PDI of Homopolymers, Diblock, and Starblock Copolymers Samples Used in Rheological Studies

sample ID	M_n (g/mol)	composition	PDI
PBBOS1	9 000	homopolymer	1.40
PBBOS2	44 700	homopolymer	1.35
diblock	18 500	PS-*b*-PBBOS 10300−8150	1.20
starblock	18 960	PS-*b*-PBBOS 9050−9910	1.22

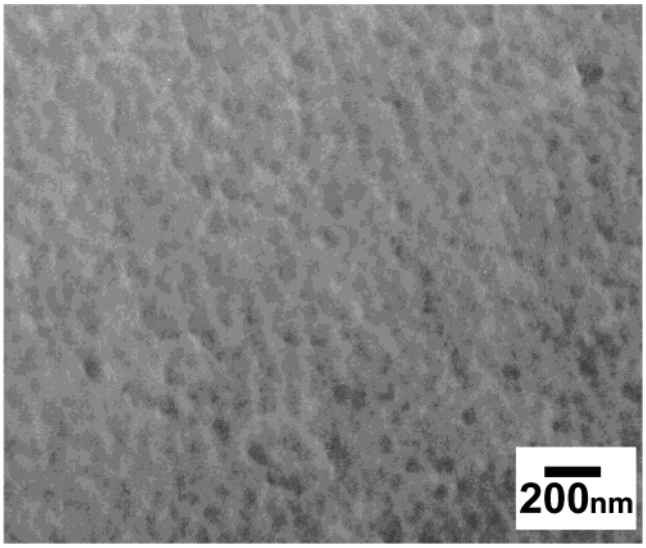

Figure 7. TEM of an unstained starblock copolymer BS1 (see Table 1). Because of packing density contrast between PS and PBBOS, PBBOS domain shows as relatively dark area in the micrograph. The scale is indicated at the right corner of micrograph.

lished in the block copolymers. On heating to 120 °C, the peak intensity gradually decreases in both block copolymers. At 150 °C, which is above the T_g of both blocks, the SAXS peak disappears in both samples. This suggests that, between 120 and 150 °C, the order−disorder transition occurs in both block copolymer samples. Fast cooling back to room temperature did not regenerate the peak, whereas slow cooling over a time period of 5−6 h did. This indicates that the microphase-separated morphology is indeed thermodynamically stable for the copolymers even though the ordering kinetics is very slow. The marginal temperature window between the T_{ODT} of the copolymers (below 150 °C) and the T_g of the PBBOS block (130 °C) can be used to rationalize the extremely slow ordering kinetics. While the diblock copolymer shows a constant SAXS peak position on heating the sample from 23 to 120 °C (Figure 6a), a marginal change in the *d* spacing from 215 to 235 Å was observed for the starblock copolymer (Figure 6b). Although the exact molecular origin for this change in *d* spacing is not known, its occurrence in only the starblock copolymers is clearly related to differences in the molecular architecture.

By using transmission electron microscopy (TEM), the local structure of the block copolymers was examined in real space. Most of the unstained samples showed oval aggregates with no long-range order corroborating the SAXS results. A typical TEM micrograph for an unstained block copolymer (BS1 in Table 1) is shown in Figure 7. The aggregates vary in size (5−60 nm) depending on the block composition. However, a precise size of these aggregates could not be calculated from TEM due to poor contrast and the lack of a preferential staining agent. In many regions the oval aggregates seem to be breaking up from lamellar regions and are most likely closer to the hockey puck two-dimensional micelle model as proposed by William and Fredricksons.[12]

Melt Rheology. As highlighted in Table 2, the two MJLCP homopolymers examined were PBBOS1 and PBBOS2 with molecular weights of 9000 and 44 700 g/mol, respectively. The diblock and starblock copolymers examined have about 50% mass fraction of MJLCP blocks and similar net LC block molecular weights as PBBOS1. MJLCPs are especially difficult systems to work with as they have a clearing temperature above their thermal degradation temperature, and hence completely erasing their thermal history is not feasible. Therefore, we have kept the thermal treatment identical for all the samples so that comparison from one sample to the other can give us reliable qualitative and some quantitative information. Each sample was measured twice, and the results were found to be reproducible. After the rheological measurements were completed, molecular weights of the samples were checked by GPC and found to be the same as before the experiments, which indicates that no significant degradation occurred during the measurements. Small shear amplitudes were used in the experiments. As a result, WAXS measurements on the samples showed no net orientation after the rheological measurements.

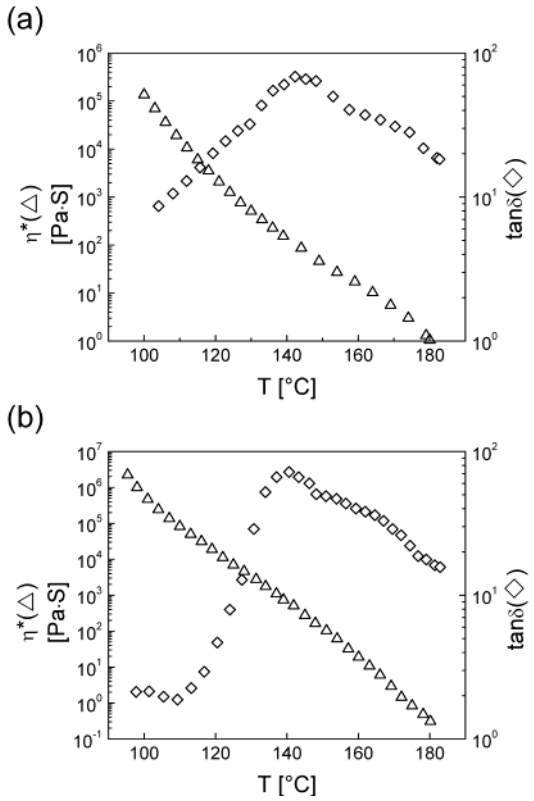

Figure 8. Temperature dependence of complex viscosity η^* (Eta*) and loss-tangent tanδ in (a) homopolymer PBBOS2 and (b) PS−PBBOS2 diblock copolymer. The data were measured at a frequency of 1rad/s. Depending on temperature, the rim strain amplitude was varied from 1% to 10% in order to obtain reasonable signal/noise ratios.

Temperature-Dependent Experiments. First, to assess effects of the thermal transitions on their rheological behavior, temperature-sweep experiments were performed on all PBBOS homopolymers and PS-*b*-PBBOS block copolymers. Over the temperature range from 95 to 180 °C, both homopolymers present similar features in the temperature dependence of their rheological behavior. The diblock and starblock copolymers, on the other hand, show almost identical temperature-sweep results. The temperature dependence of the complex shear viscosity, η^*, and loss tangent, tan δ, of a PBBOS homopolymer sample and a PS-*b*-PBBOS block copolymer are shown in parts a and b of Figure 8, respectively. No abrupt change in the complex viscosity was observed

in any of the samples, indicating the absence of a nematic−isotropic transition. This agrees with our POM observations that none of the samples go through a clearing temperature in the measured temperature range. Around 130 °C, a slight change of slope for the complex viscosity was observed in the hompolymers (Figure 8a). Correspondingly, the tan δ data present a broad peak at that temperature. For the temperature dependence of the loss tangent (tan δ) of the block copolymers (Figure 8b), there is a peak emerging at the low-temperature end, i.e., 90 °C besides the similar feature around 130 °C. These peaks at 90 and 130 °C correspond to the T_g's of PS and PBBOS, respectively, as also determined by DSC measurements. The presence of two distinct T_g's in the block copolymers is in agreement with our SAXS results that show microphase separation in these block copolymers at temperatures below 150 °C. As discussed in the previous section, the temperature-dependent SAXS measurements indicate that, in both the diblock and star block copolymers, the order−disorder transition of the microphase-separated structure should occur between 120 and 150 °C. Common rheological features related to such a transition, namely a significant decrease of moduli and increase of tan δ, do not unambiguously show up in our measurements. The reason might be that the glass transition of PBBOS blocks is in the vicinity of the order−disorder transition. A glass transition usually bears similar and even stronger rheological features than an order−disorder phase transition. Therefore, the two thermal transitions might not be distinguished in the rheological measurements of our block copolymers.

Frequency-Dependent Measurements. To investigate the dynamic fingerprint of the different molecular architectures, the frequency dependence of the rheological properties was measured at temperatures from 100 to 180 °C. For all the samples, master curves could be composed using time−temperature superposition (TTS) to retrieve the rheological responses over a wide frequency range: from 10^{-3} to 10^5 rad/s. The temperature dependence of the shift factors (a_T) could be fitted with the well-known WLF relation[14] (data not shown).

Master curves of storage (G') and loss modulus (G'') for PBBOS1 and PBBOS2 are shown in parts a and b of Figure 9, respectively. No G'/G'' crossover and/or plateau region were observed at intermediate frequencies. Thus, the entanglement molecular weight was not attained in any of the samples even though the molecular weight of PBBOS2 is 44 700 g/mol. This reflects the rigid chain conformations of the present MJLCP's. In both the homopolymer and the block copolymer samples, nonterminal behavior was observed at lower shear frequencies, consistent with the liquid crystalline nature of the present materials. In contrast to the previous study reported by Berghausen and co-workers,[13] no discontinuity was observed in the master curves. This difference is due to the fact that their system goes through a sharp nematic-to-isotropic phase transition which is absent in our system.

The effect of molecular architecture on chain dynamics becomes evident on superimposing the complex shear viscosity, η^*, and loss tangent, tan δ, data for homopolymers (PBBOS1 and PBBOS2), diblock and starblock copolymers as shown in parts a and b of Figure 10, respectively. There are two obvious trends for the complex viscosity of the samples (Figure 10a). First, when the molecular weight of the homopolymer increases from 9000 g/mol in PBBOS1 to 44 700 g/mol in PBBOS2, the viscosity drops significantly. Berghausen and co-workers have reported a similar phenomenon.[13] Considering the rigid backbone conformations in MJLCP, an increase of molecular weight results in a higher aspect ratio of the rodlike macromolecule, which is expected to enhance the nematic liquid crystallinity of the materials. Therefore, a greater extent of the MJLCP backbone alignment in the higher molecular weight sample will tend to lower the viscosity of the material under shear. Second, both block copolymers present lower complex viscosities than the homopolymer PBBOS1 even though the net molecular weight of the LC block is comparable in all three samples (∼9000 g/mol). The reduction of viscosity is most likely due to the presence of the polystyrene block. PS is in the rubbery state above its T_g (90 °C) and hence leads to a net plasticization of the polymer. It is interesting to note that the diblock copolymer has a marginally higher complex shear viscosity than its starblock counterpart. Since both block copolymers have similar net molecular weights of the MJLCP block (∼9000 g/mol), the difference is only that the LC part is split into three arms in the PS−PBBOS star block copolymer. Each arm has thus only one-third MJLCP molecular weight of that in the diblock copolymer. Following the arguments used in comparison of the complex viscosity data between PBBOS1 and PBBOS2, namely greater extent of MJLCP backbone alignment for higher molecular weight MJLCPs, contrary to what is observed experimentally, the diblock copolymer is expected to show lower complex shear viscosity than its starblock counterpart.

To thus examine the dynamics in the materials in more detail, the master curves of the loss tangent (tan δ) data are shown for all samples in Figure 10b. All the

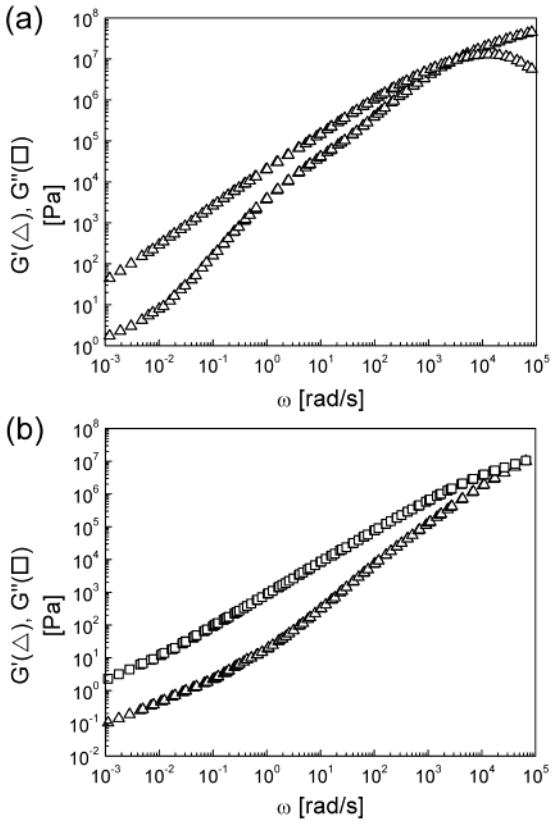

Figure 9. Master curve of storage (G') and loss modulus (G'') for (a) PBBOS1 and (b) PBBOS2 with reference temperature (T_{ref}) at 130 °C.

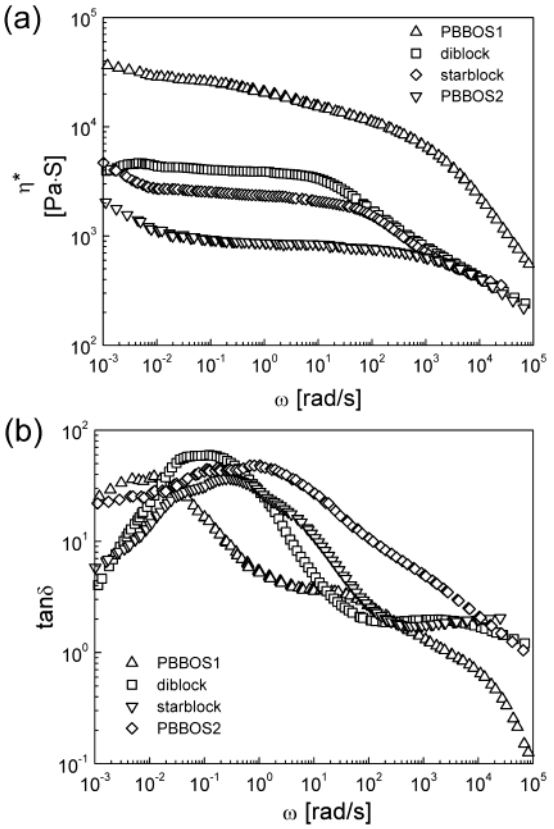

Figure 10. Master curves of (a) complex viscosity η^* and (b) loss-tangent tan δ for PBBOS1 (△), PBBOS2 (▽), diblock (□), and starblock (◇) copolymer with reference temperature at 130 °C.

samples present a broad tan δ maximum at the lower frequency end. A maximum of loss tangent is usually related to dynamic transitions from one microscopic relaxation mode to another. In the case of our MJLCP homopolymer and block copolymers, on the basis of our previous discussion, this tan δ maximum should correspond to the dynamic transition from relaxations of individual macromolecules to that of nematic LC supramolecular structures. Therefore, it may serve as a time scale mark for us to compare the effect of molecular architecture on microscopic relaxation processes in the MJLCP materials. Compared to the lower molecular weight homopolymer PBBOS1, the maximum of tan δ in all other three samples significantly shifts to higher frequencies. This indicates that the corresponding molecular relaxation times in these samples are significantly shorter than those in the homopolymer PBBOS1. Furthermore, the molecular relaxation times follow the same order as the magnitudes of the complex shear viscosities of these materials, namely PBBOS1 > diblock > starblock > PBBOS2. This observation suggests that there may be a "correlation" between the reduction of the complex shear viscosity and the decrease of the molecular relaxation times.

In our previous discussion, we have suggested that, compared with PBBOS1, the enhanced liquid crystallinity in PBBOS2 and PS plasticization in the block copolymers give rise to the reduction of the complex shear viscosity in these materials. Comparing diblock and starblock copolymers, differences of the molecular architecture can explain relatively shorter molecular relaxation times in the latter. A low molecular weight star polymer can be regarded as a branched molecule.

Table 3. Activation Energies of PBBOS Homopolymers and Their Diblock and Starblock Copolymers with Polystyrene[a]

sample	activation energy (kJ/mol)
PBBOS1	200.86 ± 16.0
PBBOS2	173.75 ± 8.5
diblock	152.08 ± 9.8
starblock	137.80 ± 6.67

[a] The values are calculated from temperature dependence of the time−temperature−superposition (TTS) shift factors (a_T).

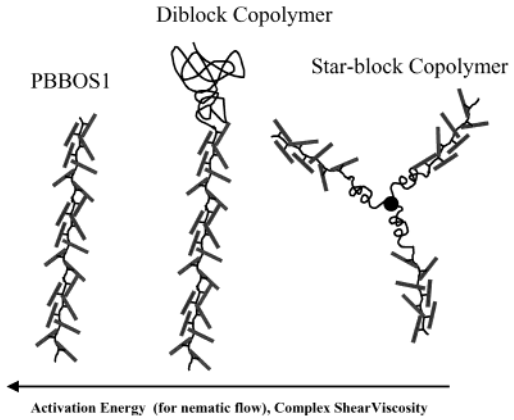

Figure 11. Cartoon depicting the molecular architecture of PBBOS1, diblock, and starblock copolymer with trends in their complex shear viscosity and relaxation times.

In general, the terminal relaxation times of a branched macromolecule are much shorter than a linear one of same molecular weight. The higher the number of branches, the larger the difference will be.[14,15a] This effect has been well studied in poly(styrene) star polymers where, for low molecular weight melts, the zero shear viscosity is found to be lower than in linear polymers of the same molecular weights.[15b,c] Similar studies are reported for star-shaped poly(isoprene).[15d] In our system the presence of three LC chain ends per molecule compared to one LC and one PS chain end in the diblock copolymer brings about a reduction in the relaxation time in the starblock.

Finally, flow activation energies were calculated from a plot of ln a_T vs $1/T$ for all the samples in their high-temperature nematic range. It allows us to compare the MJLCPs with other similar LCPs in a more quantitative manner. The results for all the samples are shown in Table 3. The values are higher than what has been reported by Berghausen and co-workers for side group polymers with laterally attached mesogens[14] and by Zentel and co-workers for end-on attached side group LCP's.[17] The differences are probably due to the fact that there are no flexible linkers in MJLCPs to decouple the motion of the side chains from that of the polymer backbone. This leads to the bulky mesogenic rods wrapping themselves around the polymer backbone, the so-called "mesogen jacketed effect". The values of the activation energies follow the same trend as exhibited by the complex shear viscosity η^* and the relaxation time derived from the tan δ data, namely PBBOS1 > diblock > starblock > PBBOS2; see also Figure 11. These results suggest that there are two ways to make MJLCPs more attractive from a processing point of view: either by enhancing nematic liquid crystallinity through higher molecular weights or by incorporating branching points, e.g., through a starlike architecture, in the molecular design.

Conclusions

Our studies show that well-defined macromolecular architectures such as diblock, triblock, and starblock copolymers can been synthesized by SFRP using a monofunctional, difunctional, or trifunctional polystyrene macroinitiator, respectively, end-capped with a TEMPO-based alkoxyamine initiator. Morphological studies on these blocks by POM and high-temperature WAXS show a nematic LC phase for most of the block copolymers which are stable up to the decomposition temperature. SAXS and TEM show the formation of microphase-separated nanostructures for the block copolymers. No significant long-range order of these structures could be detected.

The effect of varying the molecular architecture in going from homopolymers to diblock and starblock copolymers is reflected in physical properties such as complex viscosity η^* and relaxation times. No discontinuity was observed in the master curves due to the lack of a nematic to isotropic phase transition in these systems. No entanglement plateau was observed for the compositions of the block copolymers examined. The flow activation energies were found to be higher than in systems with flexible linkers between the backbone and the mesogen. There is a reduction in complex shear viscosity in going from the homopolymer BBOS to diblock to starblock copolymers attributed to the presence of the PS block leading to a plasticizing effect and to topological factors arising from the branched molecular architecture. Molecular relaxation times derived from loss tangent δ data follow the same trend as the shear viscosity. The results provide a useful synthetic strategy to tune the physical properties and hence make MJLCPs and their block copolymers more attractive from a processing point of view.

Acknowledgment. The authors thank Dr. Craig Hawker of the IBM Almaden Research Center for providing us with the macroinitiators used in this study and Anurag Jain for his help and suggestions in carrying out the rheological measurements. Funding by the Air Force Office of Scientific Research through its MURI program is gratefully acknowledged. Partial support by the Cornell Center for Materials Research (CCMR), a Materials Research Science and Engineering Center of the National Science Foundation (DMR-0079992), is appreciated. Financial support of this work by the Xerox Research Center of Canada is appreciated.

References and Notes

(1) Weissflog, W.; Demus, D. *Cryst. Res. Technol.* **1984**, *19*, 55.
(2) Lewthwaite, R. A.; Toyne, K. J. *J. Mater. Chem.* **1992**, *2*, 119.
(3) Hessel, F.; Finkelmann, H. *Polym. Bull. (Berlin)* **1985**, *14*, 375.
(4) Pugh, C.; Schrock, R. *Macromolecules* **1992**, *25*, 6593.
(5) (a) Zhou, Q. F.; Li, H. M. *Macromolecules* **1989**, *22*, 491. (b) Zhang, D.; Liu, Yuxiang.; Wan, X.; Zhou, Q. F. *Macromolecules* **1999**, *32*, 4494. (c) Tu, H.; Wan, X.; Chen, X.; Zhang, D.; Zhou, Q. F.; Shen, Z.; Ge, J. J.; Jin, S.; Cheng, S. Z. D. *Macromolecules* **2000**, *33*, 6315. (d) Mao, G.; Ober, C. K. *Handbook of Liquid Crystals*; Wiley-VCH: Weinheim, 1998; Vol. 3.
(6) Finkelmann, H.; Wendorff, H. J. Structure of Nematic Side Chain Polymers. In *Polymeric Liquid Crystals*; Blumstein, A., Ed.; Plenum Press: New York, 1985; p 295.
(7) Pragliola, S.; Ober, C. K.; Mather, P. T.; Jeon, H. G. *Macromol. Chem. Phys.* **1999**, *200*, 2883.
(8) Georges, M. K.; Veregin, R. P. N.; Kazmaier, P. M.; Hamer, J. K. *Trends Polym. Sci.* **1994**, *2*, 66.
(9) Malmstrom, E.; Hawker, C. J. *Macromol. Chem. Phys.* **1998**, *199*, 923.
(10) Tu, Y.; Wan, X.; Zhang, D.; Zhou, Q.; Wu, C. *J. Am. Chem. Soc.* **2000**, *122*, 10201.
(11) Gopalan. P.; Ober, C. K. *Macromolecules* **2001**, *34*, 5120.
(12) Williams, D. R. M.; Fredrickson, G. H. *Macromolecules* **1992**, *25*, 3561.
(13) Berghusen, J.; Fuchs, J.; Richtering, W. *Macromolecules* **1997**, *30*, 7574.
(14) Ferry, J. D. *Viscoelastic Properties of Polymers*, 3rd ed.; John Wiley & Sons: New York, 1980; p 232.
(15) (a) Zimm, B. H.; Kilb, W. R. *J. Polym. Sci.* **1959**, *37*, 19. (b) Graessley, W. W.; Roovers, J. *Macromolecules* **1979**, *12*, 959. (c) Graessley, W. W.; Roovers, J. *Macromolecules* **1981**, *14*, 766. (d) Fetters, L. J.; Kiss, A. D.; Pearson, S. D. *Macromolecules* **1993**, *26*, 647.
(16) Larson, R. *The Structure and Rheology of Complex Fluids*; Oxford University Press: New York, 1999; p 232.
(17) Zentel, R.; Wu, J. *Makromol. Chem.* **1986**, *187*, 1727.
(18) Gillmor, J. R.; Colby, R. H.; Hall, E.; Ober, C. K. *J. Rheol.* **1994**, *38*, 1623.
(19) Zhou, W. J.; Kornfield, J. A.; Ugaz, V. M.; Burghardt, W. R.; Link, D. R.; Clark, N. A. *Macromolecules* **1999**, *32*, 5581.

MA021573U